Electronic Raman Effect in Paramagnetic Crystals: $CeCl_3$

A. KIEL, T. DAMEN, S. P. S. PORTO,* S. SINGH, AND F. VARSANYI†
Bell Telephone Laboratories, Holmdel, New Jersey 07733
(Received 7 August 1968)

We present a complete study of the electronic states of the f^1 configuration of $CeCl_3$, using the electronic Raman effect. The use of this technique for studying far-infrared electronic states proved to be rather simpler than other methods, particularly when phonon states are nearby. The general features of the electronic Raman effect are discussed, including pseudovector scattering terms and asymmetric scattering intensity. Both of these latter effects have been observed in our experiments. The intensities of all lines have been calculated and are in reasonable agreement with the observations. In the case of the lines showing asymmetry in intensity, we can predict the orientation for maximum intensity as well as the magnitude of asymmetry. The phonon spectrum of $CeCl_3$ is briefly discussd. One of the phonon lines showed a small but definite asymmetry in intensity, which we are, at present, unable to explain. This particular phonon line seems to interact with the strongest electronic Raman line.

I. INTRODUCTION

THE Raman effect has a long and fruitful history as a technique for studying vibrational and rotational transitions in molecules and solids. Quite recently, considerable interest has been manifested in the electronic Raman effect of ions in solids.[1–6] Part of this has been due to the availability of optical lasers with the attendant high-spectral intensity and collimation.

The first example of the electronic Raman effect in solids was discussed in Ref. 1 where $PrCl_3$ was studied, using the 2537 Å line of mercury. In this work the electronic spectrum of the $^3H_4$, $^3H_5$, and $^3H_6$ manifolds were investigated. Of the total of 15 Raman lines expected, a total of 10 were actually observed. The absence of the other lines was probably due to the excessive width of the associated levels. No detailed investigation of relative intensities was attempted here or in other papers on the subject.

The prediction of and the basic theory of the electronic Raman effect is contained in the well-known Kramers-Heisenberg dispersion equation[7] first published in 1925. Recently, Axe[8] has analyzed two photon processes using tensor-operator techniques. This method is particularly applicable to the study of rare-earth ions in crystals. Axe considered not only the usual symmetric tensor terms but the pseudovector scattering terms[8–11] as well.

In this paper we will describe the electronic Raman effect of the Ce^{3+} system in $CeCl_3$. All of the electronic levels of the f manifold have been observed experimentally and we have attempted a complete theoretical study of this system. We believe this is the first time a complete polarization study of any electronic Raman effect has been attempted. Largely because of this we have very definitely observed two pure antisymmetric transitions forbidden by normal symmetric tensor selection rules. In addition, and perhaps more surprising, we have seen large asymmetry in the intensities of xz,zx components due to the fact that both symmetric and antisymmetric terms are allowed for these transitions.

Section II of this paper briefly reviews the theory of the electronic Raman effect with special emphasis on experimental applications. Particular attention is devoted to the origin and expected magnitudes of the pseudovector terms and some new material on intensity asymmetry is presented. Our experimental results are displayed in Sec. III. The relative intensities of all the observed lines are compared with theory with reasonably good agreement for both normal and asymmetric lines. In Sec. IV, the phonon spectrum of $CeCl_3$ is discussed and some anomalies are considered.

II. THEORY OF THE ELECTRONIC RAMAN EFFECT

The electronic Raman effect is simply an inelastic, two-photon scattering process. We can describe the interaction term between the electromagnetic field and an atomic system (in the interaction representation

---

* Present address: University of Southern California, Los Angeles.
† Present address: Ling-Temco-Vaught Corporation, Dallas, Texas.

[1] J. T. Hougen and S. Singh, Proc. Roy. Soc. (London) **A277**, 193 (1964).
[2] R. J. Elliot and R. Louden, Phys. Letters **3**, 189 (1963).
[3] J. Y. H. Chau, J. Chem. Phys. **44**, 1708 (1966).
[4] J. A. Koningstein, J. Opt. Soc. Am. **56**, 1405 (1966).
[5] J. A. Koningstein and O. Sonnich Mortensen, Nature **217**, 5127 (1968); **217**, 445 (1968).
[6] J. A. Koningstein and O. Sonnich Mortensen, J. Chem. Phys. **46**, 2811 (1967); Phys. Rev. Letters **18**, 831 (1967).
[7] W. Heitler, *The Quantum Theory of Radiation* (Clarendon Press, Oxford, England, 1954) p. 192.
[8] J. D. Axe, Phys. Rev. **136**, A42 (1962).
[9] O. Sonnich Mortensen and J. A. Koningstein, J. Chem. Phys. **48**, 3971 (1968).
[10] M. S. Childs and H. C. Languet-Higgins, Phil. Trans. Roy. Soc. London **254**, 259 (1961); **255**, 31 (1962).
[11] G. Placzek, *Handbuch der Radiologie* (Akademische Verlagsgesellschaft, Leipzig, 1934), Vol. 6, part 2, p. 205.

with time dependence removed) as

$$H_{\text{int}}=\sum_{k,\epsilon}\frac{1}{V^{1/2}}(2\pi h\nu)^{1/2}e\mathbf{r}\cdot\boldsymbol{\varepsilon}(a_k+a_k^{\dagger}),$$

where V is volume, e is electronic charge, $\boldsymbol{\varepsilon}$ is polarization vector, $\mathbf{r}$ is (x,y,z), and $a_k^{\dagger}$, a_k are creation and annihilation operators for a photon of wave vector k.

Let g and f be the initial (ground) and final states of the atomic system and i some intermediate state to which electric dipole transitions are allowed. Using straightforward second-order perturbation theory, one obtains essentially the Kramers-Heisenberg formula for the transition rate for an ion to go from state g to state f with a photon of ν_α, $\boldsymbol{\varepsilon}_\alpha$, $\mathbf{k}_\nu$ "converted" to one with ν_β, $\boldsymbol{\varepsilon}_\beta$, $\mathbf{k}_\beta$. For $E_g\equiv 0$, and ignoring the energy difference between exciting and scattered radiation (and assuming laser excitation), we obtain the transition probability

$$W(\nu)=\frac{64\pi^5\nu^3 I}{hc^4}\left|\sum_i\frac{\langle f|e\mathbf{r}\cdot\boldsymbol{\varepsilon}_\beta|i\rangle\langle i|e\mathbf{r}\cdot\boldsymbol{\varepsilon}_\alpha|g\rangle}{E_i-h\nu}+\frac{\langle f|e\mathbf{r}\cdot\boldsymbol{\varepsilon}_\alpha|i\rangle\langle i|e\mathbf{r}\cdot\boldsymbol{\varepsilon}_\beta|g\rangle}{E_i+h\nu}\right|^2 G(\nu').$$

The excitation has polarization $\boldsymbol{\varepsilon}_\alpha$, the scattered light $\boldsymbol{\varepsilon}_\beta$, I the total intensity of the input laser beam, and $G(\nu')$ the line width of the final state, $\nu'=\nu-\nu_\beta$. It is important to recognize that the sum is over *all possible* intermediate electronic states of the system. It will often be the case that for a particular intermediate state α, one of the terms in brackets is zero while the other is nonzero. For the reversed polarization, we must interchange all subscripts in the previous equation.

It is useful to introduce the quantity $P(f,g;\ \nu,\epsilon_\alpha,\epsilon_\beta)$ where the parameters are the same as above, and the first polarization $\boldsymbol{\varepsilon}$ always refers to the excitation. We define P as

$$\begin{aligned}P(f,g;\ &\nu,\epsilon_\alpha,\epsilon_\beta)\\ &=\sum_i e^2\left(\frac{\langle f|r_\beta|i\rangle\langle i|r_\alpha|g\rangle}{E_i-h\nu}+\frac{\langle f|r_\alpha|i\rangle\langle i|r_\beta|g\rangle}{E_i+h\nu}\right)\\ &\equiv\sum_i e^2\frac{1}{2}\left(\frac{1}{E_i-h\nu}+\frac{1}{E_i+h\nu}\right)\langle f|(r_\beta r_\alpha+r_\alpha r_\beta)|g\rangle\\ &\quad+\frac{1}{2}\left(\frac{1}{E_i-h\nu}-\frac{1}{E_i+h\nu}\right)\langle f|r_\beta r_\alpha-r_\alpha r_\beta|g\rangle,\end{aligned}\tag{1}$$

where $\langle f|r_\beta r_\alpha|g\rangle$ implies $\langle f|r_\beta|i\rangle\langle i|r_\alpha|g\rangle$.

The second term in (1) represents an antisymmetric scattering term which transforms like a cross product or axial vector. The first term includes the conventional symmetric terms in the Raman tensor. If we reverse the polarizations of incident and scattered beams we find that the relevent P tensor is

$$P(f,g;\ \nu,\epsilon_\beta,\epsilon_\alpha)\equiv P(f,g;\ -\nu,\epsilon_\alpha,\epsilon_\beta).\tag{2}$$

If ν is negligibly small compared to E_i, the Raman scattering is rigorously symmetric [i.e., the energy part in the second term in (1) vanishes]. It is well known that very near resonance the antisymmetric terms can become quite large. However, one has to be very far from resonance before the energy becomes negligible. For example, if $E_i=45\,000$ cm^{-1} and $h\nu=20\,000$ cm^{-1},

$$[(E_i-h\nu)^{-1}-(E_i+h\nu)^{-1}]/[(E_i-h\nu)^{-1}+(E_i+h\nu)^{-1}]=0.44.$$

Hence for many cases of interest, the relative importance of the antisymmetric terms is determined solely by the magnitude of the matrix elements $r_\beta r_\alpha-r_\alpha r_\beta$. It is sometimes stated that closure over the excited state manifolds will lead to a vanishing result for the axial terms. This, however, is strictly true only if we include *all* of the excited states manifolds. If one group lies considerably lower than the others [i.e., a $(4f^{n-1},5d)$ manifold in a $4f^n$ rare earth], closure over just this manifold will *not* lead to cancellation of $r_\alpha r_\beta-r_\beta r_\alpha$. We can demonstrate this easily, using Axe's[8,9] theory. The terms in the pseudovector Raman scattering are all proportional to the reduced matrix element

$$3\left[\frac{l(l+1)}{2l+1}\right]^{1/2}\sum_{n',l'=l\pm1}(-)^{(l-l'+1)/2}\frac{|\langle n'l'|r|nl\rangle|^2}{\Delta E(n'l')},$$

where n',l' and n,l are the principal and orbital quantum numbers of the excited and ground electronic states, respectively. If we place *all* the excited states at a constant energy E, the radial integral summations each become $\langle nl|r^2|nl\rangle$ and the sign factor leads to cancellation. Usually this is *not* appropriate since one $n'l'$ is very much lower than all the others. However if the energy of the lowest excited manifold is very high (e.g. Yb^{3+}), not only do the energy denominators act unfavorably but the tendency toward cancellation is enhanced.

It is interesting to compare the terms in Eq. (1) with the first higher-order correction to the electric dipole transition matrix. In that latter case we have matrix elements $\langle f|(\mathbf{r}\cdot\boldsymbol{\varepsilon}_\alpha)(\mathbf{r}\cdot\mathbf{k}_\beta)|g\rangle$. These can be written as $\langle f|\frac{1}{2}(r_\alpha r_\beta+r_\beta r_\alpha)|g\rangle+\langle f|\frac{1}{2}(r_\alpha r_\beta-r_\beta r_\alpha)|g\rangle$ which may be recognized as the electric quadrupole (symmetric tensor) and magnetic dipole (pseudovector) terms. Except for the energy denominators and the fact that a second polarization vector takes the place of the propagation vector, the formulation is identical. We may therefore state as a general rule that in the electronic Raman effect involving any pair of states, *antisymmetric (pseudovector) terms will occur whenever magnetic dipole transitions are allowed between those states.*

It is important to note that in the electronic Raman effect, the initial and final states are always different. This is the crucial difference between this effect and phonon Raman effect. In the latter case, we are usually in the situation where the initial and final states are identical and nondegenerate. In this case it is easy to see that axial terms are not possible,[12] $\langle j|r_\alpha r_\beta|j\rangle \equiv \langle j|r_\beta r_\alpha|j\rangle$. However, Childs[10,13] has shown that when the ground state of the crystal is degenerate, the phonon Raman effect and the Rayleigh scattering have different selection rules than in the usual nondegenerate case, including the occurrence of pseudovector transitions. Incidentally, despite the formal similarity between the Rayleigh scattering and the electronic Raman effect, the selection rules of Ref. 11 cannot be applied to our case. This is due to the fact that even if the initial and final states change in the Rayleigh scattering, they still must belong to a time-reversed pair. This is never true in the electronic Raman effect as stressed at the beginning of this paragraph. It may be interesting to note that in non-Kramers systems (even number of electrons) with a degenerate ground state, the *xy-yx* axial term always occurs in the Rayleigh scattering (except in cubic symmetry); the *xz-zx* and *yz* never occur in Rayleigh scattering). In Kramers conjugate systems (odd number of electrons), time-reversal invariance prevents the occurrence of any pseudovector terms in Rayleigh scattering.

An important situation arises when for given incident and scattered polarizations, symmetric *and* pseudovector terms occur in an electronic Raman term. This is always true for the case for *yz* or *zx* polarizations (if whenever symmetric *yz*,*xz* occur, the axial vectors S_xS_y are allowed). Since $P(f,g;\nu,\epsilon_\alpha,\epsilon_\beta)\neq P(f,g;\nu,\epsilon_\alpha,\epsilon_\beta)$, the intensity of the scattering for one setting of the polarizers ($I\approx|P|^2$) can be different in magnitude from that obtained with the opposite settings.[14] To see this more explicitly, let us apply closure over the lowest-excited manifold. Then Eq. (1) may be rewritten as

$$P(f,g;\nu,\epsilon_\alpha,\epsilon_\beta)=[(E-h\nu)^{-1}+(E+h\nu)^{-1}]S_{fg}+[(E-h\nu)^{-1}-(E+h\nu)^{-1}]A_{fg} \quad (3)$$
$$=P_S+P_A,$$

where

$$S_{fg}=\tfrac{1}{2}e^2\langle f|r_\beta r_\alpha+r_\alpha r_\beta|g\rangle,\quad A_{fg}=\tfrac{1}{2}e^2\langle f|r_\beta r_\alpha-r_\alpha r_\beta|g\rangle$$
$$P(f,g;\nu,\epsilon_\beta,\epsilon_\alpha)\equiv P(f,g;-\nu,\epsilon_\alpha,\epsilon_\beta)=P_S-P_A. \quad (4)$$

Then for $\alpha\beta$ polarization, the scattered intensity is proportional to $|P_S+P_A|^2$, while for opposite polarization, $I\approx|P_S-P_A|^2$. Since the intensity is proportional to P^2, pure antisymmetric scattering will show no asymmetry in intensity. Koningstein and Mortensen[14] predicted asymmetric scattering about the same time we first predicted and observed this effect. The maximum asymmetry occurs when $P(g,f;\nu,\alpha,\beta)=0$ or $P(g,f;\nu,\beta,\alpha)=0$. This situation occurs whenever

$$S_{fg}/A_{fg}=\pm[(E-h\nu)^{-1}-(E+h\nu)^{-1}]/[(E-h\nu)^{-1}+(E+h\nu)^{-1}].$$

An illustration of these considerations, which is in fact important to our analysis of $CeCl_3$, can be easily demonstrated. Let us take a single f electron ground state with $l=3$, $s=\frac{1}{2}$, $J=\frac{5}{2}$, $M_J=\pm\frac{5}{2}$ with a proper function denoted by $|3;\frac{5}{2},\pm\frac{5}{2}\rangle$ and an excited Raman level[12] with $l=3$, $s=\frac{1}{2}$, $J=\frac{7}{2}$, $M=\pm\frac{7}{2}$; $|3;\frac{7}{2},\pm\frac{7}{2}\rangle$. Further we assume the only excited manifold of importance is a ^2d at about 45 000 cm^{-1} with $l=2$, $s=\frac{1}{2}$ and J of $\frac{5}{2}$ or $\frac{3}{2}$. Let us determine the scattering intensity for *xz* and *zx* polarization. In this case the only excited state of interest is $|2;\frac{5}{2},\pm\frac{5}{2}\rangle$. It is easy to see that the only nonzero matrix element is $\langle 3;\frac{7}{2},\pm\frac{7}{2}|x|2;\frac{5}{2},\pm\frac{5}{2}\rangle\langle 2;\frac{5}{2},\pm\frac{5}{2}|z|3;\frac{5}{2},\pm\frac{5}{2}\rangle$. If we reverse the order of the operators we get a zero result since there is no state with $M=\frac{7}{2}$ in a ^2d manifold. If the nonzero matrix element has a value Q, the intensity of scattering for z polarized excitation, x polarized scattering if $I\sim|Q/(E-h\nu)|^2$ while for reversed polarizations $I\sim|Q/(E+h\nu)|^2$. For $E=45\,000$ cm^{-1}, $h\nu=20\,000$ cm^{-1}, that ratio of these is $(13/5)^2\simeq 6.5$, a significant asymmetry. Our observation of this effect will be described in Sec. IV.

The reader may wonder about the thermodynamic stability of the system we have just described since it appears to convert polarizations. However, it is easy to show

$$P(g,f;\nu,\epsilon_\beta,\epsilon_\alpha)=P(f,g;\nu,\epsilon_\alpha,\epsilon_\beta), \quad (5)$$

where the term on the right applies to the normal Stokes scattering and the one on the left to anti-Stokes radiation with opposite polarizations. This reciprocity condition assures that normal equilibrium is maintained even in asymmetric systems.

The differential cross section for the electronic Raman effect is given by the usual expression for second-order scattering processes.[7] For the case of $CeCl_3$ considered below we find this cross section to range from 4×10^{-31} cm^{-2} to 10^{-33} cm^{-2} (calculated values) for the transitions observed. These are an order of magnitude weaker than typical phonon Raman cross sections but are still easily observable in concentrated crystals or when resonance enhancement is feasible.

For a concise description of the electronic Raman effect in irreducible tensor-operator formalism, the reader is referred to Axe's paper.[8] In a one electron case such as Ce, it proved simpler to evaluate the matrix elements directly rather than to use effective operator techniques, particularly when using rectangular polar-

[12] Even this statement is true only to the extent one ignores the difference in frequency of exciting and scattered light.

[13] The question of anisymmetry in the phonon Raman effect and in Rayleigh scattering is considered in great detail in Ref. 10. This important paper, clearly the first to deal with crystalline materials, has not received the attention it deserves.

[14] A. Kiel, T. C. Damen, S. P. S. Porto, S. Singh, and F. Varsanyi, IEEE, J. Quant. Electron. 4, 318 (1968); J. A. Koningstein and O. S. Mortensen, Chem. Phys. Letters 1, 693 (1968).

izations. In more complicated systems, Axe's formalism is essential.

Finally, for some consideration of Frank-Condon systems and vibronic effects, the reader is referred to Ref. 9. In rare earths and, in general, for the low-lying states of any system, the Frank-Condon effect will not be important.

III. EXPERIMENTAL RESULTS

The electronic Raman effect experiments were all performed on a crystal of $CeCl_3$ using an Argon laser for the excitation source. To keep the linewidth of the electronic system small, all data was taken with a "cold-finger" liquid-helium Dewar. Several different laser lines were used (principally those at 5145 and 4765 Å) in order to eliminate any possibility of confusing Raman scattering with fluorescence from impurities. The laser beam was always directed up the axis of the Dewar while the scattering could be observed through either of two perpendicular ports. Therefore, four polarizability components could be investigated in any run. However the geometry of the crystal mounting is not exactly identical with respect to the two observation ports which leads to some error in comparing intensities. A Spex model 1400 double monochromator with a conventional detection system was used for detecting the scattering.

Selection rules for the electronic Raman effect are only slightly more complex than for the phonon Raman effect. In essence, we must replace the phonon symmetry representation by the *direct product representation* of the initial and electronic states. When the electronic states are degenerate, there will usually be several representations in the direct product and therefore rather more complex selection rules. If the electronic system has an odd number of electrons, the double valued representations must be used for the electronic states. Table I gives the selection rules for C_{3h}, symmetry, the site symmetry group of $CeCl_3$.

TABLE I. Selection rules for C_{3h}.[a] S_z, S_x, S_y are pseudovector terms ($S_z=xy-yx$, etc.), Double subscripts imply degenerate-one dimensional representations; asterisks identify double-valued representations.

$(\Gamma_1\Gamma_1)$, $(\Gamma_4\Gamma_4)$	S_z, zz, $xx+yy$
$(\Gamma_1\Gamma_{2,3})$, $(\Gamma_4\Gamma_{5,6})$	$(xx-yy, xy+yx)$
$(\Gamma_1\Gamma_4)$	...
$(\Gamma_1\Gamma_{5,6})$, $(\Gamma_4\Gamma_{2,3})$	$(S_x,S_y)(zx+xz, yz+zy)$
$(\Gamma_{2,3}\Gamma_{2,3})$, $(\Gamma_{5,6}\Gamma_{5,6})$	S_z, zz, $xx+yy$, $(xx-yy, xy+yx)$
$(\Gamma_{2,3}\Gamma_{5,6})$	$(S_x,S_y)(zx+xz, yz+zy)$
$(\Gamma_{7,8}{}^*\Gamma_{7,8}{}^*)$, $(\Gamma_{9,10}{}^*\Gamma_{9,10}{}^*)$	S_z, zz, $xx+yy$, (S_x,S_y), $(zx+xz, yz+zy)$
$(\Gamma_{7,8}{}^*\Gamma_{9,10}{}^*)$	$(xx-yy, xy+yx)$
$(\Gamma_{7,8}{}^*\Gamma_{11,12}{}^*)$, $(\Gamma_{9,10}{}^*\Gamma_{11,12}{}^*)$	$(S_x,S_y)(zx+xz, yz+zy)$
$(\Gamma_{11,12}{}^*\Gamma_{11,12}{}^*)$	S_z, zz, $xx+yy$

[a] C_{3h}: $\Gamma_1 \to A'$, $\Gamma_{2,3} \to E$, $\Gamma_4 \to A''$, $\Gamma_{5,6} \to E''$, $\Gamma_{7,8}{}^* \to E_{1/2}$, $\Gamma_{9,10}{}^* \to E_{3/2}$, $\Gamma_{11,12}{}^* \to E_{3/2}$.

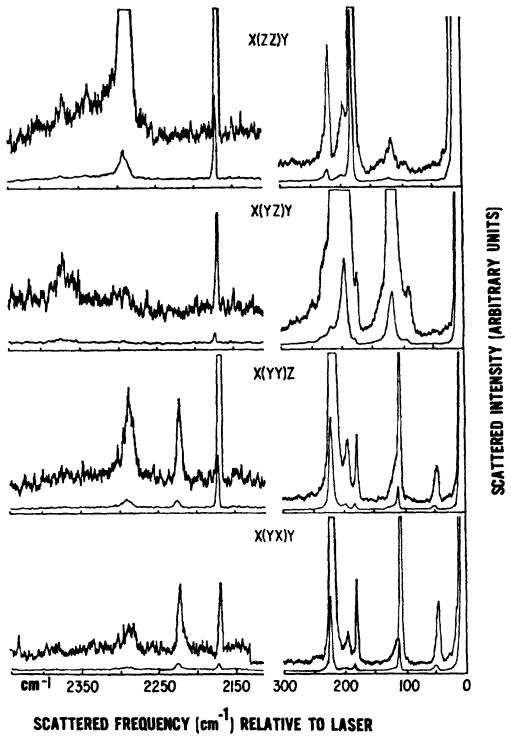

FIG. 1. Phonon and electric raman lines in $CeCl_3$. The polarizations of the lines in each row are within the parentheses, propagation directions outside the parentheses with letters to the left applying to excitation (4965 Å line of argon laser), on the right to scattering. Each chart has a low-gain and high-gain (×10) traces; wavelength should be taken from the high-gain trace. The lines on the left-hand side are all electronic ($J=\frac{7}{2}$); electronic lines at the right-hand side are at 45 cm^{-1} (xx and xy polarization) and 117 cm^{-1} (yz) polarization. Intensity of the lines at left and right cannot be compared directly.

Figure 1 shows the results of the Raman scattering using the 5145 Å line of the argon laser. The four different polarizations as shown in the column on the right. The group on the right in Fig. 1 were all the lines detected within 300 cm^{-1} of the laser excitation. This group includes the phonon lines as well as two lines we interpret as electronic Raman lines; the line at 45 cm^{-1} in yx and yy polarizations and the very strong line at 117 cm^{-1} in yz polarization. The group at the left were found in the region 2168 to 2349 cm^{-1} below the laser line. This is the region where the $^2F_{7/2}$ states of Ce^{3+} should lie. Three lines definitely appear, and we believe the broad line at 2349 cm^{-1} in yz polarization is real, accounting for the four lines expected from this manifold. We can compare these results with the results of Varsanyi for Ce^{3+} in $LaCl_3$ since $CeCl_3$ and $LaCl_3$ have identical crystal structure (C_{6h}) with very nearly identical lattice constants since Ce^{3+} and La^{3+} have about the same ionic radii. In $LaCl_3$, the site symmetry of a Ce impurity is C_{3h} so we use the site

TABLE II. Comparison of the results of the present work on $CeCl_3$ with Varsanyi and Toth's results for $LaCl_3$.[a]

	Varsanyi	Present work	Fitted
$\Gamma^*(J=\frac{7}{2}, M=\pm\frac{3}{2})$	191	200	196
$\Gamma^*(J=\frac{7}{2}, M=\pm\frac{5}{2}, \mp\frac{7}{2})$	136	119	117
$\Gamma^*(J=\frac{7}{2}, M=\pm\frac{1}{2})$	45	54	52
$\Gamma^*(J=\frac{7}{2}, M=\pm\frac{5}{2}, \mp\frac{7}{2})$	0	0	0
	(2130)	(2168)	(2168)
$\Gamma^*(J=\frac{5}{2}, M=\pm\frac{3}{2})$	112	117	119
$\Gamma^*(J=\frac{5}{2}, M=\pm\frac{1}{2})$	39	45	45
$\Gamma^*(J=\frac{5}{2}, M=\pm\frac{5}{2})$	0	0	0

[a] Reference 17.

symmetry in the comparison below.[15,16] Table II compares our results on $CeCl_3$ with the $LaCl_3$ data. The first column gives the representations and the J, M values of the states as determined by Varsanyi and Toth[17] from fitting the energies given in Column II. The energies of the four upper states are all given with respect to the lowest state of the $J=\frac{7}{2}$ manifold, the energy of which is shown in parenthesis. The third column gives all the electronic Raman lines in Fig. 1. The last column gives the energy levels calculated by modifying the $LaCl_3$ spin-orbit and crystal field[18] as follows: $\delta\lambda/\lambda=+0.01$, $\delta A_2^0/A_2^0=+0.1$, $\delta A_6^6/A_6^6=0.05$, $\delta A_6^0=\delta A_4^0=0$. These changes in the fields are quite modest even for similar lattices such as $LaCl_3$ and $CeCl_3$, yet all lines can be fitted to within our instrumental error (3 cm^{-1}). Therefore our present work confirms that of Varsanyi and Toth. The predicted electronic Raman effect polarization and those observed in Fig. 1 are shown in Table III. Since our ground state is $\Gamma_{7,8}^*$, and recognizing that at the low temperature used in our experiment all Raman line emanate from this ground state, we have predicted polarizations in order of energy.

TABLE III. Observed relative intensities of polarizations in the electronic Raman effect, with calculated relative intensities in parentheses.

	xx	xy	zz	xz	zx
45 cm^{-1}	1	1			
	(1)	(1)			
117 cm^{-1}	...	...		12	1
	(<0.01)	(<0.01)		(13)	(1.7)
2168 cm^{-1}	0.4	0.08	0.5	0.045	0.35
	(0.2)	(0.1)	(0.3)	(0.025)	(0.16)
2222 cm^{-1}	0.13	0.12			
	(0.06)	(0.06)			
2287 cm^{-1}	0.35	0.16	0.7	...	0.14
	(0.4)	(0.2)	(0.7)	(<0.01)	(0.08)
2368 cm^{-1}	...	...		0.4	...
	(<0.01)	(<0.01)		(0.3)	(0.04)

45 cm^{-1} $\Gamma_{7,8}^* \rightarrow \Gamma_{9,10}^*$ xx, yy, xy

117 cm^{-1} $\Gamma_{7,8}^* \rightarrow \Gamma_{11,12}^*$ $xz, yz, (S_x,S_y), xx, yy, xy$

2168 cm^{-1} $\Gamma_{7,8}^* \rightarrow \Gamma_{7,8}^*$ $zz, xx+yy, S_z, xz, yz(S_x,S_y)$

2222 cm^{-1} $\Gamma_{7,8}^* \rightarrow \Gamma_{9,10}^*$ xx, yy, xy

2287 cm^{-1} $\Gamma_{7,8}^* \rightarrow \Gamma_{7,8}^*$ $zz, xx+yy, S_z, xz, yz(S_x,S_y)$

2368 cm^{-1} $\Gamma_{7,8}^* \rightarrow \Gamma_{11,12}^*$ $xz,yz(S_y,S_y), xx, yy, xy$.

The polarization for the 45 cm^{-1} line agrees with prediction. In the 117 cm^{-1} line the xx,yy,xy components are missing. However, calculation shows that these components should indeed be unobservably weak, since they are nonzero only by virtue of the slight mixing of the state $|\frac{7}{2}, \pm\frac{7}{2}\rangle$ into the ground state by the crystal field. The mixing coefficient is 0.014 in $CeCl_3$ leading to a reduction in intensity of 10^{-3}. The line at 2168 cm^{-1} is the sharpest line in the spectrum, as it should be (it is instrument broadened in Fig. 1). Note that it appears in all polarizations *including* the xy case. This component can only be accounted for by the pseudovector S_z term[19] in the polarizability. The 222 cm^{-1} lines agree with the predictions while the lines at 2287 cm^{-1} are essentially the same as those at 2168 cm^{-1}. The broad line near 2368 cm^{-1} can only be reliably seen in xz polarization. This again agrees with computations which predict the xz component to be 65 times as strong as the xx,xy. Therefore, from a general point of view the agreement of our experimental results with theory is very good if we accept the pseudovector S_z term in the 2168 cm^{-1} and 2287 cm^{-1} lines. The xz component does not appear in the 2287 cm^{-1} line and is weak in the 2168 cm^{-1} line. Since we expected both these lines to be quite strong we were led to search for asymmetry in the intensity. In Fig. 2 we show most of the polarizations except that zy polarization replaces xz. Note that there are striking differences in the relative sizes of the zy polarizations in the 117, 2168, and 2287 cm^{-1} lines. The latter two are much stronger relative to the zz lines, while the 117 cm^{-1} is now relatively much weaker. This asymmetry in the intensity we attribute to the existence of the pseudovector S_x,S_y terms. Note that these observed asymmetries cannot be accounted

[15] In $CeCl_3$, the ground state is to a good approximation a pure $J=\frac{5}{2}$, $M=\pm\frac{5}{2}$ state. However, the final state in the Raman transition is a mixture of $J=\frac{7}{2}$, $M=\pm\frac{7}{2}$ and $J=\frac{7}{2}$, $M=\mp\frac{5}{2}$. This does not affect the calculated asymmetry; only the absolute intensity is changed.

[16] We shall show later that the site symmetry is often the appropriate one and, indeed, this is the case in $CeCl_3$.

[17] F. Varsanyi and B. Toth, Bull. Am. Phys. Soc. 11, 242 (1966).

[18] From Varsanyi's work the crystal fields in terms of spherical harmonics $Y_k^q(\theta,\Phi)$ is $V=A_2^0Y_2^0(\theta,\Phi)+A_4^0Y_4^0(\theta,\Phi)+A_6^0Y_6^0(\theta,\Phi)+A_6^6[Y_6^6(\theta,\Phi)+Y_6^{-6}(\theta,\Phi)]$ with $A_2^0=175$ cm^{-1}, $A_4^0=-398$ cm^{-1}, $A_6^0=-706$ cm^{-1}, $A_6^6=466$ cm^{-1} and λ (spin-orbit parameter) $=617$ cm^{-1}.

[19] Koningstein and Mortensen appear to have observed an antisymmetric transition in E_u^{2+} in garnet (Ref. 5). However, contrary to these authors' claim, J is not a good quantum number in this system since the $J=1$ level observed is only $\sim$500 cm^{-1} from the $J=2$ and the crystal-field interaction is strong. This will clearly result in large-scale mixing of the two states $M=+1$ and $M=-1$. For these states then, symmetric Raman scattering is possible, but no symmetric term can connect the $M=0$ state to the ground state ($J=0$, $M=0$).

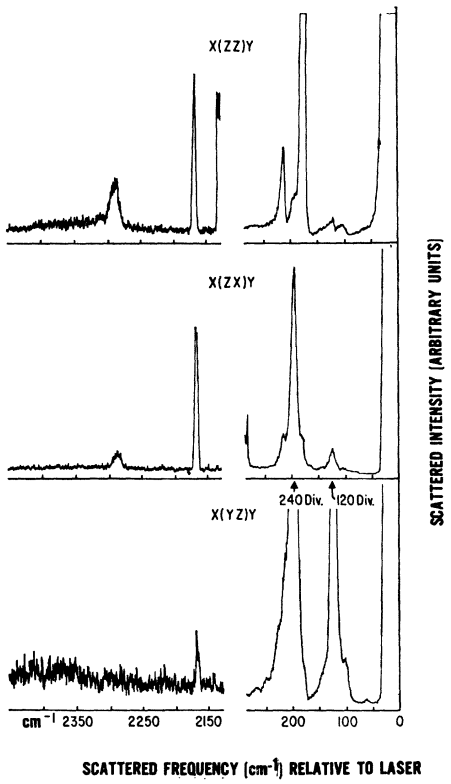

FIG. 2. Asymmetry in the electronic raman effect. The gain of the lowest trace at the left-hand side is three times as great as the upper two at the left. The 4765-Å argon laser line was used in this case.

for by differences in collection efficiency since we are comparing them to xx or yy lines which have identical geometry relative to the crystal and Dewar. Differences in relative intensity of a factor of 2 is the most one could expect. We are therefore quite confident our interpretation is essentially correct and that the theory is as expressed in Sec. II. This is the first observation of asymmetric intensity in Raman scattering.

In Table III we have collected the calculated and observed intensities for all the lines seen in Figs. 1 and 2. In both cases all intensities are integrated and normalized to those of the 45 cm^{-1} line which is *defined* as unity. In the calculation we have considered only the interaction with the d manifold at 45 000 cm^{-1}. For the observed intensities we have taken into account the grating efficiency as a function of wavelength and polarization, photo tube efficiency, the input polarizer, and differences in slits and gain. There are, therefore, considerable differences between the intensities given in the table and the relative amplitudes seen in Figs. 1 and 2. In the majority of cases the calculated and observed relative intensities are within a factor of 2. Rather more gratifying is the fact that for the lines which should show asymmetric intensities in xz or zx *we predict the correct orientations for the maxima and minima in every case.*

The major problem arises in trying to understand the large strength of the xx components of the 2168 and 2287 cm^{-1} lines. As pointed out in Sec. II, the rectangular selection rules only hold if the Kramer's pair of states are degenerate *and* are coherent (i.e., have wave functions which are in phase). In $CeCl_3$ however there is a large dipole magnetic which is rapidly varying. The phase memory time of a state in this system is less than $\approx 10^{-10}$ sec and the dipolar width of the ground state will be $\sim 10^{-1}$ cm^{-1}. Therefore each state of a Kramer's pair scatters independently although we cannot resolve them. In all cases except the xx scattering, this leads to a reduction in absolute intensity of a factor of 2. However, for the xx scattering, the incident beam propagates along the y axis, the scattered beam along the z axis. Hence in the scattered beam we are observing circular components belonging to both the xx scattering *and* the xy. The result is an increase of a factor of 3 in the intensity of the observed xx scattering.

This property of magnetic crystals will have a very important consequence in many cases of concentrated crystals. For in a majority of cases the crystal has more than one ion per unit cell with the result that the local site symmetry is lower than the crystal symmetry. If the ions do not interact, we expect the scattering to be characteristic of the space group of the crystal, i.e., coherent scattering. However, if the magnetic noise in the crystal breaks this coherence, the ions scatter independently and the site symmetry is displayed in the Raman scattering.

IV. PHONON SPECTRUM

$CeCl_3$ and $PrCl_3$ have the same structure as $LaCl_3$ as well as very similar lattice parameters. The unit cell symmetry[20,21] is C_{6h} with two ions per unit cell. This implies the existence of six Raman active modes; $2A_g$ $1E_{1g}$ and $3E_{2g}$. In previous[1,22] experiments on $LaCl_3$, only five of the six Raman active lines could be identified. Hougen and Singh[3] identified the observed spectrum in $LaCl_3$ as arising from the following vibrations: $E_{2g} \rightarrow 108$ cm^{-1}, $A_g \rightarrow 179$ cm^{-1}, $E_{1g} \rightarrow 186$ cm^{-1}, $E_{2g} \rightarrow 210$ cm^{-1} and $E_{2g} \rightarrow 217$ cm^{-1}. In addition, there appeared to be a spurious doubling of the A_{1g} vibration at 77°K which was of doubtful origin.

Following a suggestion of Asawa, Satten, and Stafsudd[22] we have examined the phonon spectrum of $CeCl_3$ (Fig. 1, right) and find that the second highest mode is really an A_g and that the second lowest is really a "doublet," one E_{2g} and one A_g (see Ref. 23 for details). Table IV, reproduced from Ref. 23, summarizes the results of our study of the phonon Raman spectrum

[20] W. H. Zachariasen, J. Chem. Phys. **16**, 254 (1948).
[21] J. Murphy, H. H. Caspers, and R. A. Buchanan, Bull. Am. Phys. Soc. **7**, 545 (1962).
[22] C. K. Asawa, R. A. Satten, and O. T. Stafsudd, Phys. Rev. **168**, 957 (1968).
[23] T. C. Damen, A. Kiel, S. P. S. Porto, and S. Singh, Solid State Commun. **6**, 671 (1968).

TABLE IV. Raman-Active modes in $CeCl_3$ and $PrCl_3$.

$CeCl_3$		$PrCl_3$	
E_{2g}	106 cm^{-1}	E_{2g}	106 cm^{-1}
A_g	176 cm^{-1}	E_{2g}	179 cm^{-1}
E_{2g}	180 cm^{-1}	A_g	183 cm^{-1}
E_{1g}	193 cm^{-1}	E_{1g}	198 cm^{-1}
A_g	216 cm^{-1}	A_g	214 cm^{-1}
E_{2g}	218 cm^{-1}	E_{2g}	217 cm^{-1}

in $CeCl_3$ and $PrCl_3$. It is fairly clear that a similar system will hold for $LaCl_3$ when observed at lower temperatures.

It is conceivable that the Ce^{3+} system can act as the ground state for the phonon Raman effect. In this case, Ref. 10 predicts the occurrence of antisymmetric scattering terms. We briefly outline the results of Ref. 10. If the ground state is a degenerate state Γ, we may divide the product representation into a symmetric product $[\Gamma,\Gamma]$ and an antisymmetric produce $\{\Gamma,\Gamma\}$. Let $\Gamma_R{}^S$ and $\Gamma_R{}^A$ be the representations of the symmetric and antisymmetric parts of the polarizability tensor and Γ_P the representation of the phonon. If the electronic system has an odd number of electrons (Kramer's degeneracy) we have symmetric scattering whenever the product $\Gamma_R{}^S \times \Gamma_P$ is contained in $\{\Gamma,\Gamma\}$. Since $\{\Gamma,\Gamma\}$ is equal to the identity representation in Kramer's systems there is no change in the selection rules for symmetric tensor scattering from the nondegenerate case. For Kramer's degenerate systems, antisymmetric terms arise whenever $\Gamma_R{}^A \times \Gamma_P$ is contained in $[\Gamma,\Gamma]$. In electronic systems with even number of electrons, symmetric scattering occurs when $\Gamma_R{}^S \times \Gamma_P$ is contained in $[\Gamma,\Gamma]$ while antisymmetric scattering take place when $\Gamma_R{}^A \times \Gamma_P$ is part of $\{\Gamma,\Gamma\}$.

In $CeCl_3$, this theory predicts that *all* the phonon lines can have *xy-yx* terms. However, careful inspection of our experimental results reveals that any antisymmetry of this type in the A, and E, modes is no greater than the normal "leak through." In the case of the E_2 modes, the Childs predictions would be manifested by asymmetry in the *xy* versus *yx* scattering. We have not been able to use an orientation to test this largely due to lack of crystals. The surprising feature of our experimental results is the fact that there appears to be a significant asymmetry on the E_1 mode (193 cm^{-1}) in *xz* polarization. After careful calibration of the system, there is about a factor of 2 difference in the intensity for *zx* versus *yz* scattering with no change in geometry (see Fig. 2, the apparent asymmetry is greater due to differences in grating efficiency and polarizer loss which must be accounted for). Since antisymmetric terms of this polarization are forbidden we cannot yet account for this result. There are some interesting features of this particular phonon line. It was the only phonon line in the spectrum whose width was temperature-dependent, getting very broad at room temperature. Indeed, it is by far the broadest of the phonon lines even at 10°K. Curiously, the shape of the 193 cm^{-1} E_{1g} phonon closely resembles the 117 cm^{-1} electronic Raman line (see Figs. 1 and 2). It seems, therefore, that this particular phonon interacts strongly with the Ce^{3+} system. It may be possible that the electronic system and phonons are strongly mixed although this seems unlikely considering the 76 cm^{-1} separation.

V. CONCLUSION

We found that using the electronic Raman effect as a spectroscopic tool was quite feasible. In fact, we believe we were able to detect the energy levels in the far infrared as easily by this method than by any other with the advantage of being able to check the complete tensor selection rules. This does not appear to be just a lucky choice since we have also seen all the electronic lines of the $^3H_4$ state of $PrCl_3$ and PrF_3. Some of this work will be published later.

ACKNOWLEDGMENTS

The authors profited from several illuminating discussions with Dr. John Hurrell and Dr. James Scott. Some unpublished reports of Professor J. A. Koningstein are also acknowledged.